Estimation by Doppler Radar of Curvature, Diffluence, and Shear in Cyclonic Flow

RALPH J. DONALDSON, JR. AND F. IAN HARRIS

ST Systems Corporation, Lexington, Massachusetts

(Manuscript received 14 July 1987, in final form 18 March 1988)

ABSTRACT

The potential for single-Doppler radar determination of wind field characteristics in cyclonic flow is examined. The influence of the four independent first-order derivatives of a wind field, namely curvature, diffluence, downwind shear, and crosswind shear, upon the Doppler radial velocities is studied. Simple models of wind fields containing each of the derivatives defined in natural coordinates are presented. When only one derivative is present at a time, it has been found that there are unique signatures for diffluence and downwind shear and qualitatively similar signatures for curvature and crosswind shear. With a model incorporating all four derivatives, techniques are developed for the recovery of these derivatives. A method is also presented that corrects the mean speed estimate. It is concluded that in most cases the recovery of the downwind shear, diffluence, the sum of curvature and crosswind shear, and mean wind is possible to within 5 percent of the true values.

Application of these techniques to radar data collected from Hurricane Gloria is discussed. A storm strength indicator based on shearing deformation and distance of cyclone center yielded signs of the declining trend of the storm an hour or two before this trend manifested itself significantly in the wind speed as estimated by the Doppler radar, therefore suggesting potential as a forecast tool.

1. Introduction

Wind field analysis through use of a single-Doppler radar was first suggested by Probert-Jones (1960). He observed the component of motion of snow along his radar beam at two different azimuth angles and deduced the wind speed and direction appropriate to both azimuths. The Velocity Azimuth Display (VAD) scan was offered by Lhermitte and Atlas (1961). It is a simple and efficient technique for systematic estimation of wind speed and direction when suitably reflective wind tracers surround the radar. In the VAD mode, the radar antenna is set into a conical scan about a vertical axis, at a fairly low elevation angle in order to prevent excessive contribution to the Doppler velocity measurements by precipitation fall speeds. These measurements, recorded at a particular range during a complete 360° scan in azimuth, provide information on the wind field along the VAD scanning circle at a height given by range and elevation angle.

Both Probert-Jones and Lhermitte and Atlas recognized the underlying assumption in their techniques of a horizontally uniform wind vector throughout the area of observation. Eventually the uniformity assumption was replaced by a less restrictive assumption of linearity. Browning and Wexler (1968) extended the VAD technique to a consideration of nonuniform wind fields that vary linearly in the horizontal plane. A linear wind field is also a necessary assumption in the generalized VVP method (Volume Velocity Processing) developed by Waldteufel and Corbin (1979).

The assumption of linearity utilized in all of the above estimation techniques tends to break down when intense cyclonic storms such as hurricanes are considered. Observations of such storms by ground-based Doppler radars are limited, but there are strong suggestions of nonlinear effects (e.g., Donaldson et al. 1978). Passarelli (1983) explored the opportunities for analysis by single-Doppler radar of nonlinear wind fields. Inspired by his commentary, Donaldson and Harris (1984) initiated a study to assess the effects of variable wind curvature and linear wind field gradients upon VAD patterns through simulations. Their results were encouraging and provided the motivation for this in-depth study to examine all four first-order derivatives of the winds in cyclonic flow, with curvature inversely proportional to distance from its center, and to develop methods for recovery of these derivatives, whenever possible.

2. First derivatives of the wind field

The analysis presented here considers first-order spatial derivatives of wind velocity in a horizontal plane. Because the focus of this study is upon cyclones, wherein variable curvature is likely, the derivatives are expressed most conveniently in natural coordinates referred to the streamlines. In the natural coordinate system the s-axis is tangent to a streamline with s increasing downwind, the n-axis is normal to a streamline

Corresponding author address: Mr. Ralph J. Donaldson, ST Systems Corporation, 109 Massachusetts Avenue, Lexington, MA 02173.

with n increasing to the left of the wind vector and V is wind speed at the origin of the natural coordinate axes. A change in wind direction is denoted by the angle ψ, which is positive toward the n-axis. Both speed and direction may vary along either of the coordinate axes; thus there are four independent first-order derivatives: $\partial V/\partial s$ (downwind shear), $\partial V/\partial n$ (crosswind shear), $V\partial\psi/\partial s$ (curvature), and $V\partial\psi/\partial n$ (diffluence).

It is well known (e.g., Petterssen 1956) that the kinematic properties of a wind field are given by sums and differences of its first-order derivatives. Expressed in natural coordinates, the kinematic properties are:

$$\text{Divergence} = \partial V/\partial s + V\partial\psi/\partial n \quad (1)$$

$$\text{Stretching Deformation} = \partial V/\partial s - V\partial\psi/\partial n \quad (2)$$

$$\text{Shearing Deformation} = V\partial\psi/\partial s + \partial V/\partial n \quad (3)$$

$$\text{Vorticity} = V\partial\psi/\partial s - \partial V/\partial n. \quad (4)$$

The first three of these kinematic properties may be calculated from the Doppler VAD patterns. Caton (1963) showed that divergence is the net horizontal outflow integrated throughout the radar scanning circle divided by its radius. Browning and Wexler (1968) showed how the two components of deformation can be determined from the amplitude and phase of the second-order Fourier harmonic of the Doppler VAD pattern, assuming that the wind field derivatives can be considered as constant throughout the radar scanning circle.

Our examination of the wind field derivatives is intended to provide an aid for diagnosis of hurricanes and other intense cyclonic storms. Consequently, we have expressed curvature as inversely proportional to distance from a center of curvature, as a highly simplified first approximation to flow around a cyclone. Also, we have expressed diffluence as inversely proportional to distance from a virtual streamline apex, in order to preserve streamline continuity. We shall test the range of applicability of the Browning and Wexler technique in a wind field with curvature and diffluence varying according to our simple model of cyclonic flow.

It is convenient to reference the radar observations of Doppler velocity, defined as the scalar component of wind velocity along the radar beam, to a polar coordinate system with origin at the radar, and position defined by range r and azimuth angle α. Following geographical convention, and postulating for the moment a mean westerly wind, we align the coordinate system so that the wind across the radar site is moving toward $\alpha = 90°$ and the orthogonal direction to the left of the wind is $\alpha = 0°$. Stated in Cartesian coordinates, these directions are along the x axis and y axis, respectively. For the sake of simplicity we assume that radar elevation angles and vertical motions are sufficiently small so that their neglect introduces errors of negligible importance in comparison with contributions from other sources. An estimated correction for contamination by vertical motions could be introduced, if necessary.

Figure 1 depicts each of the first derivatives, combined with uniform translation from left to right, in the context of the radar scanning circle. The radius of the radar scanning circle is r, and F and R represent distances to the centers of diffluence and curvature, respectively. Initially, we shall examine the Doppler VAD patterns specific to each one of the wind fields illustrated in Fig. 1. In later sections combinations of the wind field derivatives and their resultant VAD patterns will be studied, including the general case in which all four derivatives are present.

a. Downwind shear

Figure 2 illustrates the geometry of the radar scanning circle (dashed) of radius r observing a wind field with both downwind and crosswind shear. The wind speed at the radar site is V_0. In the case of downwind shear, the wind speed increases from a minimum of $V_0(1 - d)$ at distance r upwind from the radar to $V_0(1 + d)$ at distance r downwind from the radar. Accordingly, the shear is $V_0 d/r$. The dimensionless parameter d is defined as the fractional increase in wind speed from radar site downwind to the VAD scanning circle.

At any point on the radar scanning circle, this wind field has a speed of

$$V(\alpha) = V_0(1 + d\sin\alpha) \quad (5)$$

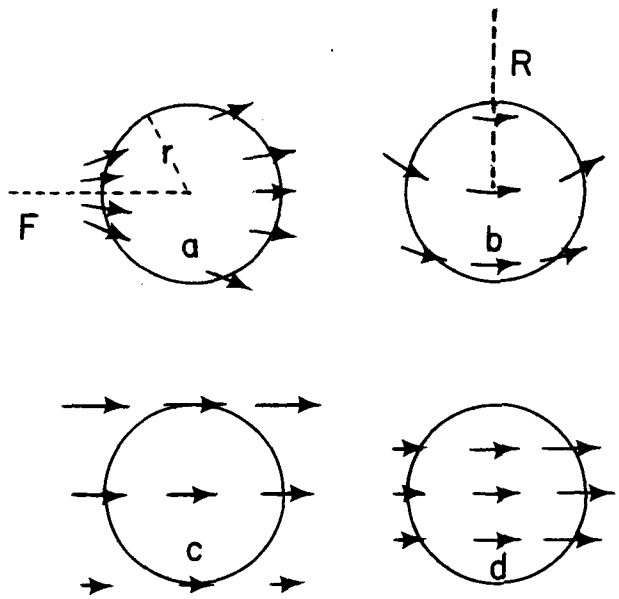

FIG. 1. Schematic depiction of the four first derivatives of the horizontal wind field: (a) Diffluence, (b) Curvature, (c) Crosswind shear, and (d) Downwind shear. Each derivative is superimposed on a radar scanning circle of radius r. Arrows indicate wind vectors representing the sum of a derivative and a constant translation toward the right of each sketch. (From Ruggiero and Donaldson 1987).

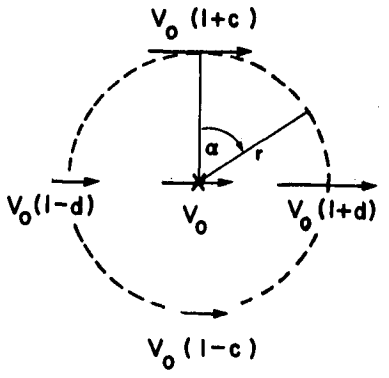

FIG. 2. Schematic depiction of linear wind field model with both downwind and crosswind shear. Arrows represent wind vectors, dashed line is radar scanning circle of radius r, with location on circle given by azimuth angle α. (From Donaldson and Harris 1984).

and a uniform direction toward $\alpha = 90°$. Accordingly, the Doppler velocity V_D, the component of wind along the radar beam, is

$$V_D(\alpha) = V(\alpha)\sin\alpha = V_0(\sin\alpha + d\sin^2\alpha). \quad (6)$$

A visual examination of the VAD pattern readily reveals the presence of downwind shear by noting a difference in magnitude of the maximum and minimum values of Doppler velocity. These extrema occur at $\alpha = 90°$ and 270°, respectively, for the simple case of downwind shear expressed in Eq. (6), yielding a straightforward method for evaluation of d:

$$d = [V_D(\max) + V_D(\min)]/[V_D(\max) - V_D(\min)]. \quad (7)$$

b. Crosswind shear

The wind speed at any point on the radar scanning circle for the case of pure crosswind shear, with uniform wind direction toward $\alpha = 90°$, is

$$V(\alpha) = V_0(1 + c\cos\alpha). \quad (8)$$

The shear toward the left of the wind direction is V_0c/r, where c is the dimensionless parameter of crosswind shear and is defined as the fractional increase in wind speed over a distance r normal and to the left of wind direction. Under these conditions the Doppler velocity measured by the radar is

$$V_D(\alpha) = V(\alpha)\sin\alpha = V_0(\sin\alpha + c\sin\alpha\cos\alpha). \quad (9)$$

The most prominent effect of crosswind shear on a visual display of the Doppler VAD pattern is a deviation from diametric opposition of the locations of the maximum and minimum Doppler velocities. Unfortunately, the cause of this effect is not unique, because later discussion will demonstrate that a curved wind field produces a pattern rather similar in appearance. Figure 3 illustrates this deviation, which is measured by the angle δ_D on the downwind side of the pattern, and δ_U on the upwind side. (The ϵ angles will be discussed later in the section on diffluence.)

The δ angles are useful for an immediate visual recognition of the presence of crosswind shear and/or curvature. Also, in cases where data coverage is not complete around the VAD circle but the δ angles are clearly displayed, their magnitude provides a qualitative indication of the combined effects of crosswind shear and curvature. For example, if crosswind shear is the only wind field derivative, $\delta_D = \delta_U$, and these angles may be determined by differentiation of (9) with respect to α to find the angular locations of the Doppler velocity extrema, which have a complementary relationship to the two identical δ angles. This process yields

$$\sin\delta = [(1 + 8c^2)^{1/2} - 1]/4c \quad (10)$$

and can also be expressed more compactly as

$$c = \sin\delta/\cos2\delta. \quad (11)$$

Note that c and δ have the same sign in (10) and (11), and therefore the Doppler velocity extrema are displaced toward the direction of positive crosswind shear.

c. Curvature

Following the discussion of Donaldson and Harris (1984), we have assumed that curvature is inversely proportional to distance from a center of curvature that has a fixed position relative to the radar location. This assumption of variable curvature but fixed center of curvature has two distinct advantages: it provides a simple depiction of wind field curvature around a cyclone, and it defines geometric relationships between the wind field and the radar scanning circle that enable calculation of Doppler velocities by straightforward trigonometric manipulation.

The geometry of a radar scanning a curved wind field is portrayed in Fig. 4. (Ignore for the moment

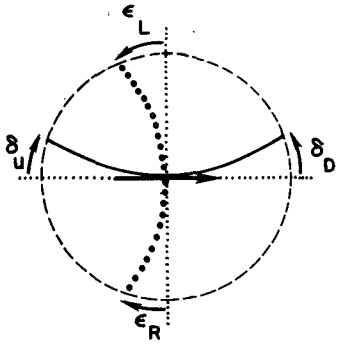

FIG. 3. Illustration defining the angles δ_D, δ_U, ϵ_L, and ϵ_R. Dashed line is radar scanning circle; dotted lines indicate directions along and normal to wind vector (arrow) at the radar; solid line is locus of minimum or maximum Doppler velocity; small circles show locus of zero Doppler velocity.

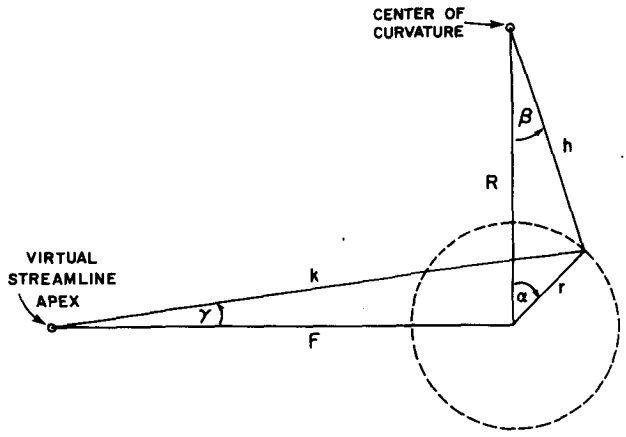

FIG. 4. Portrayal of geometric relationships required for specification of curvature and diffluence and their Doppler velocities. Dashed line is radar scanning circle, with α as the azimuth angle of any arbitrary point on this circle. R and h, with inclusive angle β, are distances from center of wind field curvature to radar and to the arbitrary point on the radar scanning circle, respectively. F and k, with inclusive angle γ, are distances from virtual streamline apex to radar and to the same arbitrary point, respectively.

distances F and k and angle γ; these will enter our discussion of diffluence in the next section.) The distance r is the radius of the radar scanning circle and R is the distance from the radar to the center of curvature of the wind field. The radar scanning angle α is oriented so that the center of curvature is in the direction $\alpha = 0°$. The wind direction at the radar site is toward $\alpha = 90°$, appropriate to cyclonic curvature in the Northern Hemisphere. The variable h is the distance from center of curvature to any point on the radar scanning circle. This point is also located by the angle β measured from the line R joining the center of curvature and the radar. The angle β is positive for the downwind semicircle, where $0° < \alpha < 180°$. Our analysis requires the assumption that $r < R$, and this is easily granted because r is under human control. The wind speed V_0 is assumed uniform.

The curved wind field can be expressed in Cartesian coordinates as the vector sum of components u and v, where u is directed along $\beta = 90°$ and v along $\beta = 180°$. Inspection of Fig. 4 readily shows that $u = V_0 \cos\beta$ and $v = V_0 \sin\beta$. The radar can detect motion only along its beam. Accordingly, at any location on the radar scanning circle the Doppler velocity V_D is given by wind components along the direction α. Therefore,

$$V_D(\alpha) = u \sin\alpha + v \cos\alpha$$
$$= V_0(\sin\alpha \cos\beta + \cos\alpha \sin\beta). \quad (12)$$

Through trigonometric solution of the right triangle in Fig. 4 that has h as hypotenuse and β as one of its angles, and after some algebraic manipulation, we find that $h = R\rho^{1/2}$, so that (12) can be expressed simply as a function of radar scanning angle α and a dimensionless parameter r/R relating the radii of radar scanning circle and curvature:

$$V_D(\alpha) = \rho^{-1/2} V_0 \sin\alpha, \quad (13)$$

where $\rho = 1 + (r/R)^2 - 2(r/R)\cos\alpha$. Note that $V_0 \sin\alpha$ in (13) is the VAD pattern of a uniform linear wind directed toward $\alpha = 90°$, so the factor $\rho^{-1/2}$ is the modification of the VAD effected by curvature varying inversely with distance to the center of curvature.

The increment of direction per unit distance along a streamline ($\partial\psi/\partial s$) for a circularly curved wind field is the inverse of the radius of curvature. Consequently, the curvature term appearing in (3) and (4) is evaluated in our model wind field as $V_0/h = V_0/R\rho^{1/2}$ at any point on the radar scanning circle. The curvature term at the radar site, where $r = 0$ and ρ reduces to unity, is simply V_0/R.

The effect of curvature on the Doppler VAD pattern is qualitatively similar to the effect of crosswind shear: the maximum and minimum Doppler velocities are displaced toward the center of curvature. The effect is illustrated by the δ angles of Fig. 3. If curvature is the only wind field derivative, the upwind and downwind δ angles are equal and may be determined by differentiation of (13) with respect to α. An alternate and simpler method for calculation of δ starts with the reflection that the extrema in the VAD pattern of a curved wind field without speed gradients occur at the two angles where the wind direction is aligned with the radar beam. Therefore, the angular locations of the extrema are obtained by setting $V_D = \pm V_0$ in (13) and solving for α. The solution is $\cos\alpha = r/R$, and since δ is complementary with the angular location of a maximum or minimum in the VAD pattern,

$$r/R = \sin\delta. \quad (14)$$

d. Diffluence

Diffluence, like curvature, is characterized by nonuniform wind direction. Unlike curvature, the diffluent directional shift is along a line normal to a streamline. Heretofore, the quantitative measurement of diffluence by a single Doppler radar has not been considered explicitly, although Baynton et al. (1977) showed that the presence of diffluence is very easily recognized in a Doppler VAD pattern by an asymmetric locus of zero-Doppler velocity. Since the zero-Doppler locus indicates wind directions normal to the radar beam, any deviation of the two branches of this locus from opposition at the same range reveals a cross-flow difference in wind direction at the corresponding height.

A field of constant translation with constant diffluence as its only derivative does not appear to be a realistic possibility within a horizontal plane. We were not able to envision continuous streamlines through a uniformly diffluent field unless the streamlines were also curved, with curvature increasing with the cu-

mulative effect of diffluence. Consequently, we have selected a diffluence model in which linear streamlines radiate from a fictitious virtual streamline apex. The diffluent wind vectors are sketched in Fig. 1(a), and geometrical relationships of the virtual streamline apex with the radar scanning circle are depicted in Fig. 4. The distance from streamline apex to radar is F, and to any point on the radar scanning circle is k. The angle between the F and k lines is γ, considered positive in the counterclockwise direction. The coordinates r and α of the radar scanning circle are identical to the case for curvature, with coordinate axes aligned so that wind direction at the radar site is toward $\alpha = 90°$.

An expression for a diffluent wind field and its Doppler velocity measured by a radar in VAD scanning mode can be generated in a manner analogous to the derivation employed in the previous section for our curved wind field model. The variable diffluent wind field can be expressed in Cartesian coordinates as the vector sum of components u and v, where u is directed along $\gamma = 0°$ and v along $\gamma = 90°$. In the absence of shear the wind speed has a uniform value V_0, and with wind direction dependent only on diffluence, Fig. 4 shows that $u = V_0 \cos\gamma$ and $v = V_0 \sin\gamma$. Since the radar detects motion only along its beam, the Doppler velocity V_D at any point on the radar scanning circle is given by wind components along the beam direction α. Therefore,

$$V_D(\alpha) = u \sin\alpha + v \cos\alpha$$
$$= V_0(\sin\alpha \cos\gamma + \cos\alpha \sin\gamma). \quad (15)$$

Substitution for γ in (15) may be accomplished by trigonometric solution of the right triangle in Fig. 4 that has k as hypotenuse and γ as one of its angles. It is helpful to express $k = F\phi^{1/2}$, where $\phi = 1 + (r/F)^2 + 2(r/F)\sin\alpha$. By means of these manipulations, (15) may be expressed as a function of radar scanning angle α and a dimensionless parameter r/F relating radius of the radar scanning circle r to the distance F from radar to the virtual streamline apex:

$$V_D(\alpha) = \phi^{-1/2} V_0(\sin\alpha + r/F). \quad (16)$$

Note that (16) reduces to the VAD pattern of a uniform linear wind directed toward $\alpha = 90°$ when F is infinitely distant, indicating a condition of zero diffluence. Also, for a confluent, or negatively diffluent, wind field the virtual streamline apex would be downwind or to the right of the radar in Fig. 4, and F would be considered negative.

The diffluence term in Eqs. (1) and (2), $V\partial\psi/\partial n$, may be evaluated in either of two ways. In our diffluent model wind field, diffluence is dependent only on distance k from the virtual streamline apex. This condition requires that $\partial\psi/\partial n$ be constant along any curve normal to a streamline. Therefore we can easily integrate ψ from 0 to ψ_1. The corresponding integration for n is a circular arc length with angle ψ_1 and radius equal to distance k on Fig. 4 from any given point on the radar scanning circle to the virtual streamline apex. Accordingly, the diffluence term is $V_0\psi_1/\psi_1 k = \phi^{-1/2}V_0/F$, recalling that $k = F\phi^{1/2}$. At the radar site ϕ reduces to unity and the diffluence term is simply V_0/F.

The other method for evaluating diffluence is calculation of divergence under the condition of uniform wind speed V_0, which requires $\partial V/\partial s = 0$ in Eq. (1). We can do this by calculating the net outflow from a small area of width Δs with curved sides everywhere normal to the diffluent wind field and subtending an angle ψ_1. In our diffluent wind field model we set the radius of one curved side as k and the other (downwind) side as $k + \Delta s$. In this way we relate the calculation of divergence to radar parameters, because k terminates at any arbitrary point on the radar scanning circle. The inflow to this curved area is $V_0 k\psi_1$ and outflow is $V_0(k + \Delta s)\psi_1$, with no flow across the narrow sides of width Δs because these sides are oriented along the direction of flow. The size of the area in question is infinitesimally larger than $k\psi_1 \Delta s$. Consequently the divergence, and also the diffluence, is $[V_0(k + \Delta s)\psi_1 - V_0 k\psi_1]/k\psi_1 \Delta s = V_0/k = \phi^{-1/2}V_0/F$, which is identical to the previous calculation.

The easily recognizable signature of diffluence in the Doppler VAD pattern is a departure from opposition of the locus of zero Doppler velocity on either side of the mean wind vector, as illustrated in Fig. 3 by the angles ϵ_L and ϵ_R. Subscripts L and R denote the deviation from normal to the mean wind on its left and right sides. Diffluence is indicated by skewing upwind of the zero Doppler locus, as depicted in Fig. 3. A skewing downwind of the zero Doppler locus would indicate confluence, in which case the ϵ angles would be considered negative by our convention. In the absence of curvature, the two ϵ angles are equal, regardless of the presence or absence of crosswind and/or downwind shear.

The ϵ angles may be easily evaluated by solving Eq. (16) for α_0, the zero-crossing angles of the radar scan. For all values of $(r/F) < 1$, $\phi > 0$ and the solution is $\sin\alpha_0 + r/F = 0$. From our definition of ϵ as portrayed in Fig. 3, $\epsilon_L = -\alpha_{0_L}$ and $\epsilon_R = \alpha_{0_R} - \pi$. Consequently $\sin\epsilon = -\sin\alpha_0$ and

$$r/F = \sin\epsilon. \quad (17)$$

This is a useful relationship for achieving a quick estimate of the sign and magnitude of diffluence from a cursory examination of the Doppler VAD pattern, because the Doppler velocity changes most rapidly with radar scanning angle at a zero crossing. On this account the zero crossing angle is least likely to be affected by small-scale perturbations in the wind field.

3. Combination of curvature and crosswind shear

Donaldson and Harris (1984) examined the interesting combination of curvature and crosswind shear,

in which both derivatives are readily recognized by a δ signature in the VAD pattern, as given by Eq. (10) or (11), and (14), and both derivatives contribute to the shearing deformation. This earlier analysis, with slightly different notation, is reproduced here. As in the previous section, we postulate flow around a cyclone, with curvature varying inversely with distance from the center of circulation.

In combination with curvature, the crosswind shear has a variable direction because it is normal to the curved streamlines and directed toward the center of curvature. However, the wind vector and its Doppler velocity may be defined through the geometry of Fig. 4. The wind speed at any point on the VAD circle is a linear function of $h = R\rho^{1/2}$, the distance from center of wind field curvature to an arbitrary location observed by the radar. The speed function may be determined by assigning $V = V_0$ at the radar and noting, through Eq. (8), that $V(h) = V_0(1 + c)$ for $\alpha = 0°$; and at this point on the radar scanning circle Fig. 4 shows that $r = R - h$. Accordingly,

$$V(h) = V_0[1 + c(R - h)/r]$$
$$= V_0[1 + c(r/R)^{-1}(1 - \rho^{1/2})]. \quad (18)$$

The direction of the wind field is identical to the case of curvature without shear, so the Doppler velocity of the curvature–crosswind shear combination is similar to (13), but with $V(h)$ substituted for V_0:

$$V_D(\alpha) = \rho^{-1/2}V_0[1 + c(r/R)^{-1}(1 - \rho^{1/2})] \sin\alpha. \quad (19)$$

A remarkable simplification of (19) occurs in the case of solid rotation, wherein rotational speed increases linearly with distance from the center of curvature. If the radar scanning circle is entirely within the region of solid rotation (e.g., within the area bounded by the eye wall of a hurricane), we may write $V_0/R = V_0(1 + c)/(R - r)$, which reduces to

$$c(\text{solid rotation}) = -r/R. \quad (20)$$

Substitution of this relationship into (19) reduces its bracketed factor to $\rho^{1/2}$, finally leaving $V_D(\alpha) = V_0 \sin\alpha$. Within solid rotation, the effects on Doppler velocity of curvature and crosswind shear cancel exactly, and the resultant VAD pattern is identical to that observed with pure translation.

Potential vortex flow, with wind speed inversely proportional to distance from a cyclone center, is another regime of special interest. This type of flow may be a better approximation to a hurricane wind field, beyond the radius of maximum wind speed, than is a linear crosswind shear.

In potential vortex flow the product of wind speed around a circulation center and distance from this center is constant. Consulting Fig. 4, then, we see that the wind speed at any point on the radar scanning circle is

$$V(\alpha) = V_0R/h = V_0\rho^{-1/2}, \quad (21)$$

where, as before, V_0 is wind speed at the radar location. The Doppler velocity, with wind field direction identical to the case of curvature, is given by (13) with wind speed function (21) substituted for the constant speed V_0 of (13):

$$V_D(\alpha) = \rho^{-1/2}V_0\rho^{-1/2} \sin\alpha = \rho^{-1}V_0 \sin\alpha. \quad (22)$$

Differentiation of (22) with respect to α reveals, as expected, considerably greater deviation of the Doppler velocity extrema from the mean wind vector, than in the simple relationship (14) for curvature with uniform wind speed:

$$\sin\delta = 2(r/R)/[1 + (r/R)^2]. \quad (23)$$

4. An approximation for the combination of all four wind field derivatives

When both curvature and diffluence are present the simple trigonometric relationships of Fig. 4 for either curvature or diffluence alone are not valid. The lines F and R joining the radar location with virtual streamline apex and center of curvature, respectively, are no longer straight, and the angles γ and β are no longer defined in terms of right triangles. Also, these two angles are interdependent. An exact solution for the wind field and its Doppler velocity could not be derived. Therefore, approximations were sought relating β and γ to radar parameters. By inductive reasoning, we proposed that

$$\sin\beta \approx (k - F)/h \quad \text{and} \quad \sin\gamma \approx (R - h)/k \quad (24)$$

would be reasonable approximations, retaining the definitions for $h = R\rho^{1/2}$ and $k = F\phi^{1/2}$ used in the earlier analysis of single derivatives, with ρ as before equal to $1 + (r/R)^2 - 2(r/R)\cos\alpha$ and $\phi = 1 + (r/F)^2 + 2(r/F) \times \sin\alpha$.

The approximations stated in (24) approach equality as $F \gg r$ (for $\sin\beta$) and as $R \gg r$ (for $\sin\gamma$). Reference to Fig. 4 shows that each approximation converges to its exact independent form as the other term vanishes. That is, $(k - F) \to r \sin\alpha$ as $F \to \infty$ and $(R - h) \to r\cos\alpha$ as $R \to \infty$. At the approach of these limits, the centers of rotation and diffluence are separated by 90° as seen from the radar.

We propose now to use the approximations of (24) to develop an expression for the VAD pattern when all four wind field derivatives of our model are present. We will then test the accuracy of the wind field derivatives recoverable by Fourier analysis from this expression, and suggest a range of parameter values wherein the Browning and Wexler technique can be used for successful practical analysis of cyclonic wind fields that may incorporate nonuniform derivatives.

The angles β and γ indicate the changes in wind direction owing to curvature and diffluence, respectively. When both of these derivatives are present, but with no shear, the Doppler velocity of the VAD pattern is

$$V_D(\alpha) = V_0 \sin(\alpha + \beta + \gamma), \quad (25)$$

where, as before, V_0 is wind speed at the radar site. Substitution of the approximations of (24) into (25) eventually yields an expression for the Doppler velocity with both curvature and diffluence present, but with no shear. This expression is stated in terms of the radar coordinates r and α and the dimensionless parameters r/R and r/F of curvature and diffluence:

$$V_D(\alpha) \approx V_0 \sin\{\alpha + \sin^{-1}[(r/R)(r/F)^{-1}(\phi^{1/2} - 1)\rho^{-1/2}] + \sin^{-1}[(r/F)(r/R)^{-1}(1 - \rho^{1/2})\phi^{-1/2}]\}. \quad (26)$$

The next step in the problem is approximation of the two shears when there is both curvature and diffluence. Consider first downwind shear. Along the curved streamline that crosses the radar location, an expression is required for streamline length from radar to scanning circle. The product of downwind shear $V_0 d/r$ and the length of this curved streamline segment defines the wind speed at the points where this central streamline intersects the radar scanning circle. Finally, a general expression is required for wind speed at any point on the radar scanning circle, reducible to the simple expression $V(\alpha) = V_0(1 + d \sin\alpha)$ for linear, parallel streamlines as both curvature and diffluence approach zero.

The distance along a curved streamline from radar location to scanning circle is only slightly greater than the radius r of the scanning circle. In fact, it can be demonstrated that the difference is only 1% for the fairly large value of $r/R = 0.5$. Even at the limiting value of $r/R = 1$, the difference is only 5%. Consequently, the approximation of r for streamline distance from radar to scanning circle is acceptable for all permissible values of r/R. By a similar argument, r is a suitable approximation, throughout all permissible values of r/F, for distance from the radar location to the intersection of the radar scanning circle with the streamline–normal curve for diffluent streamlines.

Next, a reasonable approximation is made for distance downwind from radar location to *any* point on the radar scanning circle, and distance crosswind (in the left direction) to this same arbitrary point. From Fig. 4 it appears that $k - F$ approximates well the downwind distance, and $R - h$ is a good approximation for the crosswind distance. Since $k - F \to r \sin\alpha$ as $F \to \infty$ and $R - h \to r \cos\alpha$ as $R \to \infty$, these approximations merge smoothly toward the linear values wherein curvature and diffluence approach zero.

It is now possible to express wind speed at any point on the radar scanning circle in terms of radar coordinates and the dimensionless parameters of the wind field derivatives. The increase in wind speed from radar to scanning circle is the appropriate shear multiplied by the appropriate distance. Accordingly,

$$\text{downwind} \quad V(\alpha) \approx V_0 + (V_0 d/r)(k - F). \quad (27)$$

Similarly,

$$\text{crosswind} \quad V(\alpha) \approx V_0 + V_0(c/r)(R - h). \quad (28)$$

The wind speed at any point on the radar scanning circle is given by wind speed at the radar multiplied by the product of the two shear-dependent factors implicit in (27) and (28). Also, substitution of $R\rho^{1/2}$ for h and $F\phi^{1/2}$ for k reduces all variables to radar coordinates and parameters of the wind field derivatives. Finally, substitution of the resultant speed function for V_0 in (26) provides a general approximation for Doppler velocity when all four derivatives of our model wind field are present. The final expression is

$$V_D(\alpha) \approx V_0[1 + c(r/R)^{-1}(1 - \rho^{1/2})] \times [1 + d(r/F)^{-1}(\phi^{1/2} - 1)] \times \sin\{\alpha + \sin^{-1}[(r/R)(r/F)^{-1}(\phi^{1/2} - 1)\rho^{-1/2}] + \sin^{-1}[(r/F)(r/R)^{-1}(1 - \rho^{1/2})\phi^{-1/2}]\}. \quad (29)$$

It is necessary to demonstrate that (29) reduces to one of the exact forms (13) or (16) when either diffluence or curvature is not present and there is no shear, or to (6) or (9) when both curvature and diffluence are absent but either downwind or crosswind shear is present. With zero diffluence, $r/F = 0$ and $\phi^{1/2} = 1$. Simple substitution of these values in (29) would result in 0/0 in two of its factors. In order to avoid this indeterminacy, basic considerations are required. Recall that $\phi = 1 + (r/F)^2 + 2(r/F)\sin\alpha$. As diffluence approaches zero, F approaches very large values, at which $\phi \approx 1 + 2(r/F)\sin\alpha$, $\phi^{1/2} \approx 1 + (r/F)\sin\alpha$, and $(r/F)^{-1}(\phi^{1/2} - 1) \approx \sin\alpha$. Similarly, as curvature approaches zero and R approaches very large values, $(r/R)^{-1}(1 - \rho^{1/2}) \approx \cos\alpha$. Therefore, for zero diffluence but finite curvature, the directional factor $\sin\{—\}$ in (29) reduces to $\sin\{\alpha + \sin^{-1}[(r/R)\rho^{-1/2}\sin\alpha]\}$, and through a trigonometric identity this can be written in a form equivalent to (12) and eventually simplified to (13). Through a similar process it can be demonstrated that, with zero curvature but finite diffluence, the directional factor $\sin\{—\}$ in (29) reduces to $\sin\{\alpha + \sin^{-1}[(r/F)\phi^{-1/2}\cos\alpha]\}$ and eventually simplifies to (16). When both curvature and diffluence are zero, the directional factor reduces all the way down to $\sin\alpha$ and the speed factors are greatly simplified also. As a result of these simplifications, the exact solutions for the special cases of zero diffluence and/or curvature follow:

With zero diffluence,

$$V_D(\alpha) = V_0[1 + c(r/R)^{-1}(1 - \rho^{1/2})] \times [1 + d\sin\alpha]\rho^{-1/2}\sin\alpha. \quad (30)$$

With zero curvature,

$$V_D(\alpha) = V_0[1 + c\cos\alpha] \times [1 + d(r/F)^{-1}(\phi^{1/2} - 1)]\phi^{-1/2}(\sin\alpha + r/F). \quad (31)$$

With neither curvature nor diffluence,

$$V_D(\alpha) = V_0[1 + c\cos\alpha][1 + d\sin\alpha]\sin\alpha. \quad (32)$$

It is satisfying to note that (30) with $d = 0$ is identical to (19), which was derived along an approach somewhat different from the reasoning behind (30).

The validity of the general approximation (29) may be tested for any arbitrary combination of the dimensionless parameters (c, d, r/R, r/F) of the four wind field derivatives (crosswind shear, downwind shear, curvature, and diffluence). The method of testing first requires synthesis of the Doppler velocity function $V_D(\alpha)$ for a complete VAD circle by insertion of the arbitrary parameter values in (29). The next step is a Fourier analysis of the synthesized $V_D(\alpha)$ function, using the method developed by Browning and Wexler (1968). The Fourier coefficients of zeroth, first, and second order are a_0, a_1 and b_1, and a_2 and b_2, respectively. In performing this analysis care is taken to assure that the wind vector at the radar location is directed toward $\alpha = 90°$. With this precaution, b_1 estimates the mean wind speed around the VAD scanning circle and $a_1 = 0$ or very nearly so. Divergence is given by a_0/r, stretching deformation by $-2a_2/r$, and shearing deformation by $2b_2/r$. (The negative sign for the coefficient in stretching deformation is a result of our clockwise rotation of radar scanning angle α.) We can now insert these Fourier estimates in the basic wind field relationships (1), (2), and (3), multiply all terms by r, and divide all terms by V_0, using b_1 as an estimate for V_0, to obtain

$$a_0/b_1 = d + r/F, \quad (33)$$

$$-2a_2/b_1 = d - r/F, \quad \text{and} \quad (34)$$

$$2b_2/b_1 = r/R + c. \quad (35)$$

The final step in testing is a comparison of the left sides of (33) to (35), obtained by Fourier analysis of (29), with the appropriate combinations of the arbitrarily selected true values of wind field parameters on the right sides. Results of testing over a wide universe of parameter values ($-0.1 \leq c \leq 0.4$, $-0.3 \leq d \leq 0.1$, $-0.1 \leq r/F \leq 0.3$, and $0 \leq r/R \leq 0.8$) indicated errors of less than 5% for $r/R = 0.6$ or less and for r/F and d of opposite sign. Moreover, the validity of the approximation (29) was verified, even for r/R as large as 0.8, by continuity of the calculated Fourier coefficients b_1 and b_2 for all concurrent values of r/F, including $r/F = 0$ for which an exact formulation (30) of $V_D(\alpha)$ is applicable. Consequently, we have demonstrated that the technique of Browning and Wexler may be used for suitably accurate kinematic analysis of the wind field around a cyclone in which the magnitude of curvature varies inversely with distance from the center of curvature.

Results from testing our model indicate that, whenever variable curvature and/or variable diffluence are present, the Fourier coefficients are underestimated. These errors tend to cancel in the ratio of coefficients on the left sides of (33) to (35). However, wind speed, as estimated by b_1, may be greatly underestimated: by 20 percent or more, for example, with $r/R = 0.8$. On the other hand, the mean magnitude of the two extrema of Doppler velocity $V_m = [V_D(\max) - V_D(\min)]/2$ usually considerably overestimates wind speed in the presence of variable curvature and/or variable diffluence. Consequently, it was found empirically that the best estimate of wind speed is $(b_1 V_m)^{1/2}$. Within our universe of parameter value calculations, $(b_1 V_m)^{1/2}$ averaged only 1% high, and all of the $(b_1 V_m)^{1/2}$ values were in error by less than 5%.

5. Application to hurricane diagnosis

The techniques developed in the foregoing discussion are well adapted for estimation of the wind field derivatives in hurricanes, and may aid in detection of changes in hurricane intensity before evidence of such trends becomes apparent through local wind speed measurements. In application of this goal, the coordinate axes are aligned with the observed wind direction so that $\alpha = 90°$ is mean downwind, and the Fourier harmonics are calculated and entered in (33), (34), and (35). The sum and difference of (33) and (34) provide Fourier estimates of the parameters of downwind shear and diffluence. Accordingly,

$$d = (a_0 - 2a_2)/2b_1, \quad \text{and} \quad (36)$$

$$r/F = (a_0 + 2a_2)/2b_1. \quad (37)$$

Care must be taken, of course, to minimize observational errors, following the recommendations of Browning and Wexler (1968).

Unfortunately, there is no straightforward method for apportionment of the parameters of curvature and crosswind shear from their sum in (35). However, if we make the simple assumption that curvature of the wind field is inversely proportional to distance from a circulation center (for example, a hurricane eye), and if this distance R can be estimated reasonably well, we can solve (35) for $\tilde{c}$, defined as the parameter of *normative crosswind shear* that is required under this assumption as a contribution to the measured shearing deformation. The distance R from radar to circulation center is generally available for hurricanes, because the eye locations of threatening hurricanes are usually monitored at frequent intervals by aircraft and/or satellite. Therefore,

$$\tilde{c} = 2b_2/b_1 - r/R. \quad (38)$$

The normative crosswind shear is obtained by multiplying its parameter in (38) by V_0, the wind speed at the radar, and dividing by r, the radius of the VAD scanning circle. Accordingly, normative crosswind shear is

$$\tilde{c}V_0/r = (2b_2/b_1 - r/R)(b_1 V_m)^{1/2}/r, \qquad (39)$$

using $(b_1 V_m)^{1/2}$ as the best available estimate for V_0, where $V_m = [V_D(\max) - V_D(\min)]/2$. In cyclonic storms, wherein curvature normally increases with decreasing distance to circulation center, the normative crosswind shear accounts for this increase and therefore is not subject to the dependence of the shearing deformation on the varying contribution of curvature owing *solely* to distance from radar to circulation center.

Ruggiero and Donaldson (1987) examined the trend of wind field derivatives in Hurricane Gloria during its 1985 journey across New England, using measurements recorded by the AFGL radar at Sudbury, MA. The radius of the VAD circle was 40 km, with elevation angle 1.0° and height above radar 800 m. Their most interesting result, depicted in Fig. 5, was a comparison of normative crosswind shear with wind speed at the radar.

Before landfall of Hurricane Gloria its maximum reported wind speed was 65 m s^{-1}, and warnings were issued about the devastation that could be inflicted if winds of such speed reached land. Fortunately, the hurricane had weakened by the time of landfall. Figure 5 shows that normative crosswind shear was observed to be near zero at 1600 UTC when Gloria entered Long Island, and actually decreased during the next 3 h to less than -2×10^{-4} s^{-1} as the hurricane approached. This is a surprising result, because crosswind shear in a normal hurricane would be expected positive toward the ring of maximum velocity surrounding the eye. However, if circulation around the hurricane decayed and the actual curvature parameter was reduced on that account to values substantially below r/R, a small positive crosswind shear could still be maintained even with negative values of *normative* crosswind shear. Evidently this was the case in Hurricane Gloria's encounter with New England: after the eye region entered the unambiguous velocity range of the radar, no signature of rotation could be detected. Also, as distance from radar to the hurricane center decreased from 251 km to 103 km over a 3 h period, Fig. 5 indicates that wind speed at the radar increased by only 15%, suggesting a positive crosswind shear but with much smaller magnitude than would be expected in an active hurricane. During the final half hour of the VAD measurements, wind speed actually decreased slightly.

This analysis of Hurricane Gloria led Ruggiero and Donaldson (1987) to propose that the normative crosswind shear (39) might be operationally applied as a Storm Strength Indicator, or SSI. For example, in a normally active hurricane we might expect that wind speeds would increase by at least 10 m s^{-1} as distance toward the eye wall decreased by 100 km. If circulation around the normally active hurricane supports a curvature field with magnitude varying inversely with distance from circulation center, the measured SSI would be at least 10^{-4} s^{-1}. Therefore, values of SSI $< 10^{-4}$ s^{-1}

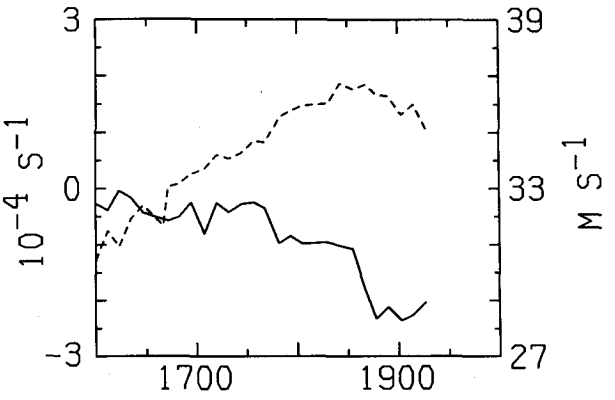

FIG. 5. Trend of wind speed (dashed curve, right-hand scale) and normative crosswind shear (solid curve, left-hand scale) at 800 m altitude in Hurricane Gloria (1985), derived from Doppler VAD measurements from AFGL radar at Sudbury, MA. Time scale along abscissa is in UTC. During these measurements the distance from radar to circulation center decreased from 251 km to 103 km. (Adapted from Ruggiero and Donaldson 1987.)

suggest a storm of less than vigorous strength, and negative values of SSI probably indicate a decay of both circulation and wind speed. The example of Hurricane Gloria showed promise for forecasting the intensity of a storm advancing toward the radar. The measurement of SSI near zero at landfall, and trending negative thereafter, was confirmed by a negative trend in wind speed at the radar more than 2 h later.

In conclusion, the trend in Hurricane Gloria of the Storm Strength Indicator is an encouraging development for monitoring the intensity of circularly configured storms at distances remote from the radar site. This indicator may provide clues to the behavior of an advancing storm an hour or two before confirming information on wind speeds is measured at the radar. After the establishment of the NEXRAD system, this technique should be especially useful in assessing the threat to coastal areas by offshore hurricanes as well as intense extratropical storms.

6. Summary

The four first-order spatial derivatives of a wind field are curvature, diffluence, downwind shear, and crosswind shear. In cyclonic flow, these derivatives are most conveniently expressed in natural coordinates referred to the streamlines. Divergence, vorticity, stretching deformation, and shearing deformation are kinematic properties comprised of sums and differences of pairs of the wind field derivatives. All of these properties except vorticity may be calculated by Fourier analysis of the Doppler velocity function measured by a radar scanning a complete circle in azimuth at constant range, following the VAD analysis technique proposed by Browning and Wexler (1968). The recovery of each of the wind field derivatives when one or more of them are variable in cyclonic flow, however, is not a straight-

forward proposition, and this question was explored in depth.

Simple models of each wind field derivative in turn were considered with a Doppler radar scanning in the VAD mode inserted into the wind field, in order to synthesize characteristic Doppler velocity functions of radar scanning angle. The models for curvature and diffluence do not have constant values throughout the wind field. Instead, the curvature is defined to be a variable, an inverse function of distance from a circulation center. A novel approach was used to model diffluence, by postulating a virtual (but fictitious) streamline apex. The synthesized Doppler velocity functions for each of the wind field derivatives reveal unique signatures for diffluence and downwind shear, but qualitatively similar signatures for curvature and crosswind shear.

For the natural, realistic situation wherein all four of the modeled wind field derivatives are present, an exact solution could not be found for the resultant Doppler velocity function. However, a suitable approximation was derived that reduced to an exact solution when either curvature or diffluence, or both, were eliminated. The validity of the approximation was tested over a wide-ranging set of parameter values of the four derivatives. For each set a Doppler velocity function was synthesized and then analyzed for the Fourier harmonics, which were then compared with the appropriate sums and differences of the derivatives. Results of the test showed that errors in recovery of the wind field derivatives were less than 5% except for unusual cases with diffluence and downwind shear not of opposite sign, or fairly high values of curvature for which distance from radar to center of curvature is less than twice the radius of the radar scanning circle. The test also revealed a substantial underestimate of wind speed by the magnitude of the first Fourier harmonic whenever diffluence and/or curvature were present. However, the square root of the product of this first harmonic and mean magnitude of the Doppler velocity extrema significantly reduced the error to a few percent. Consequently, there is confidence in most cases for the recovery from natural wind fields of downwind shear, diffluence, and the sum of curvature and crosswind shear, as well as wind speed.

A storm strength indicator (SSI), proposed earlier by Ruggiero and Donaldson (1987), is suggested as a promising index for remote and early detection of trends in hurricane intensity. In conditions suitable for Fourier analysis of the VAD pattern, the SSI is given by the shearing deformation minus an estimated curvature term that is inversely proportional to distance from radar to circulation center. During measurements conducted in New England in Hurricane Gloria (1985), the SSI showed decay after landfall of both circulation and wind speed toward the eye region an hour or two before confirmation by other, more direct radar measurements. This type of diagnosis, conducted at a radar located on a coast, should be helpful in providing advance warning of the threat by destructive offshore cyclones.

Acknowledgments. We are pleased to take this opportunity to express our gratitude for the extensive assistance provided by our former colleague, Frank H. Ruggiero (now with AFGL). He programmed the Doppler velocity patterns for a wide variety of wind field models, provided Fourier analyses for these patterns, devised interpolative and averaging techniques for analysis of Doppler velocities in natural wind fields, and offered suggestions for the analysis of the Hurricane Gloria dataset. We are also grateful for data on this hurricane acquired by the AFGL Doppler radar at Sudbury, MA, under the direction of Kenneth M. Glover. A dedicated team of AFGL engineers and technicians deserve our highest appreciation for their successful round-the-clock efforts to complete major radar repairs in time to permit data acquisition in Hurricane Gloria. This team included Graham Armstrong, Alexander Bishop, T Sgt Richard Chanley, Edward Duquette, Douglas Forsyth (now at NSSL), 1st Lt Allan Sadoski and William Smith. We gratefully acknowledge the valuable criticisms and suggestions offered by a reviewer. Finally, we wish to thank Mrs. Sundie Meroth and L. A. McLaughlin for their careful efforts in preparing our manuscript. This work was supported under AFGL Contract F19628-82-C-0023.

REFERENCES

Baynton, H. W., R. J. Serafin, C. L. Frush, G. R. Gray, P. V. Hobbs, R. A. Houze, Jr. and J. D. Locatelli, 1977: Real-time wind measurements in extra-tropical cyclones by means of Doppler radar. *J. Appl. Meteor.*, **16**, 1022–1028.

Browning, K. A., and R. Wexler, 1968: The determination of kinematic properties of a wind field using Doppler radar. *J. Appl. Meteor.*, **7**, 105–113.

Caton, P. G. F., 1963: Wind measurement by Doppler radar. *Meteor. Mag.*, **92**, 213–222.

Donaldson, R. J., Jr., M. J. Kraus and R. J. Boucher, 1978: Doppler velocities in rain bands of Hurricane Belle. Preprints, *18th Conference on Radar Meteorology,* Atlanta, Amer. Meteor. Soc., 181–184.

Donaldson, R. J., Jr., and F. I. Harris, 1984: Detection of wind field curvature and wind speed gradients by a single Doppler radar. Preprints, *22nd Conference on Radar Meteorology,* Zurich, Amer. Meteor. Soc., 514–519.

Lhermitte, R. M., and D. Atlas, 1961: Precipitation motion by pulse Doppler. Proceedings, *Ninth Weather Radar Conference,* Kansas City, Amer. Meteor. Soc., 218–223.

Passarelli, R. E., Jr., 1983: Wind field estimation by single Doppler radar techniques. Preprints, *21st Conference on Radar Meteorology,* Edmonton, Amer. Meteor. Soc., 526–529.

Petterssen, S., 1956: *Weather Analysis and Forecasting, Volume I.* 2nd ed. McGraw-Hill, 428 pp.

Probert-Jones, J. R., 1960: Meteorological use of pulsed Doppler radar. *Nature,* **186,** 271–273.

Ruggiero, F. H., and R. J. Donaldson, Jr., 1987: Wind field derivatives: A new diagnostic tool for analysis of hurricanes by a single Doppler radar. Preprints, *17th Conference on Hurricanes and Tropical Meteorology,* Miami, Amer. Meteor. Soc., 178–181.

Waldteufel, P., and H. Corbin, 1979: On the analysis of single-Doppler radar data. *J. Appl. Meteor.*, **18**, 532–542.